

Molecular mechanism of CAIF inhibiting myocardial infarction by sponging miR-488 and regulating AVEN expression

XIAOLING LI¹, RUNQI CHEN¹, LINA WANG¹, ZENGXUE LU², YANGJIE LI¹ and DUN TANG¹

¹Intensive Care Unit, Guilin People's Hospital, Xiangshan 541002; ²Department of Gastroenterology, Xing'an County People's Hospital, Xing'an, Guilin, Guangxi 541300, P.R. China

Received October 12, 2020; Accepted June 30, 2021

DOI: 10.3892/mmr.2022.12786

Abstract. In recent years, the global incidence and mortality of myocardial infarction (MI) has increased and become one of the important diseases threatening public health. Long non-coding (lnc)RNAs are a type of ncRNA that serve critical roles in the progression of various types of disease. The present study aimed to investigate the effect and mechanism of lncRNA cardiac autophagy inhibitory factor (CAIF) on cardiac ischemia/reperfusion (I/R) injury. CAIF was down-regulated in the myocardium of I/R rats and cardiomyocytes treated with hydrogen peroxide (H₂O₂). Further experiments demonstrated that CAIF overexpression inhibited I/R-induced cardiac infarction and apoptosis *in vivo*. CAIF decreased H₂O₂-induced apoptosis and oxidative stress of cardiomyocytes. Mechanistically, CAIF sponged microRNA (miR)-488-5p; this interaction was confirmed by rescue experiments. Moreover, miR-488-5p targeted apoptosis and caspase activation inhibitor (AVEN) and inhibited its expression. In summary, the present data identified a novel CAIF/miR-488-5p/AVEN signaling axis as a key regulator of myocyte apoptosis, which may be a potential therapeutic target for the treatment of MI.

Introduction

Myocardial infarction (MI) is ischemic necrosis of myocardial tissue (1). It is the leading cause of death globally and ~20% of patients experiencing an MI die within 1 year of the event (2). Thus, restoring blood supply as early as possible is key to decrease infarction volume and protect cardiac function. Restoring blood supply is termed reperfusion in acute MI treatment (3). However, reperfusion/reoxygenation worsens myocardial tissue injury, known as ischemic-reperfusion (I/R) injury (4,5).

Long non-coding (lnc)RNAs, a class of ncRNA, are more >200 bp in length. lncRNAs were once considered to exhibit no biological function due to unclear functions and species (6). With the development of high throughput sequencing technology, the functions of lncRNAs have been identified (7-9). lncRNAs are involved in a number of regulatory processes, including chromosomal dose compensation, genomic imprinting, epigenetic regulation, cell differentiation and stem cell maintenance (10-12). Abnormalities in lncRNAs are associated with cardiovascular disease in humans (13). Evidence suggests that lncRNAs are involved in the regulation of myocardial apoptosis (14-16). However, the effect of lncRNAs on regulation of myocardial apoptosis remains unclear. Cardiac autophagy inhibitory factor (CAIF) is a novel discovered lncRNA (17). CAIF suppresses MI by targeting the p53/myocardin-dependent autophagy pathway (18). In addition, CAIF is down-regulated in end-stage cardiomyopathy (19). However, the precise role and underlying mechanisms of CAIF remain to be determined.

MicroRNAs (miRNAs/miRs) are single-stranded, nc endogenous RNA 18-25 nucleotides in length that negatively regulate gene expression post-transcription (20,21). miRNAs serve an important role in a variety of physiological and pathological processes, including embryonic development (22,23), cell proliferation and differentiation (24,25), apoptosis, metabolism and tumorigenesis (26). Studies have reported differential expression of miRNAs in MI including, miR-19a/19b, miR-21, miR-206 and miR-483 (27,28).

Apoptosis and caspase activation inhibitor (AVEN) is an anti-apoptotic protein that controls apoptosis partially by abrogating caspase activation via binding to Bcl-xL and apoptotic peptidase activating factor (Apaf)-1. AVEN was demonstrated to mediate the protective effect of miR-30b-5p on hypoxia-induced cardiomyocyte injury (29).

The present study aimed to explore the role of CAIF in MI progression. Cardiomyocytes were treated with 200 μ M H₂O₂ for 4 h to establish cardiomyocyte injury *in vitro* and female C57BL/6 mice were purchased for MI model establishment *in vivo*. Flow cytometry and TUNEL assays were performed to analyzed cell apoptosis. CAIF, miR-488-5p and AVEN levels were measured by PCR or western blot. The present study may provide a potential target for the diagnosis of infarct heart diseases.

Correspondence to: Dr Dun Tang, Intensive Care Unit, Guilin People's Hospital, 12 Wenming Road, Xiangshan 541002, P.R. China
E-mail: feu2875@163.com

Key words: long non-coding RNA, cardiac autophagy inhibitory factor, microRNA-488, myocardial infarction

Materials and methods

Mouse model of MI. A total of 24 female C57BL/6 mice (weight, 20.12±1.28 g; age, 12 weeks) were purchased from Beijing Vital River Laboratory Animal Technology Co., Ltd. (Beijing, China) and housed in a 12/12-h light/dark cycle at 22-26°C and 50-70% humidity with *ad libitum* access to food and water. The mice were divided into Sham, I/R, I/R + Ad-nc and I/R + Ad-CAIF groups (all n=6). For I/R treatment, mice were anesthetized with 1% pentobarbital (60 mg/kg) and were intubated and attached to a small animal ventilator. Following thoracotomy, the intercostal muscle was separated in the 3rd and 4th intercostal space to expose the heart. The middle of the left anterior descending coronary artery was ligated with a 5-0 surgical suture. Following 30 min ischemia, the surgical suture was removed for reperfusion. Mice were euthanized with intraperitoneal injection of 3% pentobarbital (180 mg/kg). Cessation of breathing and loss of the righting reflex were considered to indicate mortality. The mice in the I/R + Ad-nc group were injected with 100 μ l Ad-nc via the tail vein, and the mice in the I/R + Ad-CAIF group were injected with 100 μ l Ad-CAIF 7 days before I/R. The mice in the sham group were only exposed by thoracotomy without ligation. In the I/R group, the heart was harvested at 0, 1, 4 or 8 h after reperfusion for the further analysis. The study was approved by the Ethics Committee of Guilin People's Hospital.

Isolation of primary cardiomyocytes. A total of 10 female neonatal mice (weight, 19.58±1.34 g; age, 1-3 days) were purchased from Beijing Vital River Laboratory Animal Technology Co., Ltd. and euthanized using CO₂ (displacement rate, 60% volume/min) followed by cervical dislocation according to AVMA guidelines (30). Cessation of breathing and movement were considered to indicate mortality. Then, the mice were sterilized with alcohol and the heart was removed. Then, 1 0.10% collagenase and 1 ml 0.08% trypsin were added into a 15 ml centrifuge tube. The chopped tissue was digested at 37°C for 10 min and centrifuged at 4°C (710.4 x g, 10 min). After that, the supernatant was discarded to remove endothelial cells. Then, 1 ml 0.1% II collagen proteinase was added to the 15 ml tube and digested for 10 min at 37°C. After centrifuging at 4°C (710.4 g, 10 min), the supernatant was transferred to a new 50 ml centrifuge tube and 1 ml DMEM/F12, supplemented with 10% FBS (both Procell), was added. This process was repeated 6-7 times. The cell suspension was centrifuged at 4°C and 200 x g for 5 min, then cells were collected and inoculated into a sterile 35-mm petri dish and cultured for 120 min (37°C, 5% CO₂). The non-adherent cells were inoculated into a new gelatin-coated petri dish (DMEM/F12 supplemented with 10% FBS) and cultured for 24 h (37°C, 5% CO₂) to obtain cardiomyocytes.

H₂O₂ treatment. As oxidative stress injury is an important part of I/R injury (31). H₂O₂ was used to simulate oxidative injury in cardiomyocytes. Cardiomyocytes were treated with 200 μ M H₂O₂ for 4 h at 37°C to establish cardiomyocyte injury, as previously described (32,33).

Oligonucleotide transfection. Adenovirus overexpressing CAIF (Ad-CAIF), small interfering CAIF (si-CAIF) and their

negative control were obtained from Hanbio Biotechnology Co., Ltd. miR-488-5p mimic and mimic control (50 nM), inhibitor and inhibitor control (50 nM) were purchased from Shanghai GenePharma Co., Ltd. Oligonucleotides were transfected using a Lipofectamine[®] 3000 kit (Invitrogen; Thermo Fisher Scientific, Inc.) according to the manufacturer's instructions at room temperature. At 48 h post-transfection, cells were harvested for subsequent experiments. Sequences were as follows: miR-488-5p mimic: 5'CCCAGATAATGG CACTCTCAA3'; mimic control: 5'CCTGAGTCCGACAAT TACGTAC3'; miR-488-5p inhibitor: 5'TTGAGAGTGCCA TTATCTGGG3' and inhibitor control, 5'CTAGGGATA CCGTTTATCATAAC3'.

Reverse transcription-quantitative (RT-q)PCR. RNA was extracted from tissue and cells using an Beyozol RNA extraction kit (Beyotime Institute of Biotechnology) according to the manufacturer's instructions. A total of 500 ng RNA was reverse-transcribed into cDNA using a Reverse Transcription kit (Takara Bio, Inc.) according to the manufacturer's instructions. RT-qPCR was performed using a SYBR-Green kit (Takara) and a PCR Detection system (Applied Biosystems) according to the manufacturer's instructions. The RT-qPCR conditions consisted of initial denaturation at 95°C for 30 sec, followed by 40 cycles of denaturation at 95°C for 5 sec and annealing at 60°C for 30 sec. The expression of miR-488-5p was normalized to U6, while the expression of CAIF and AVEN mRNA were normalized to GAPDH. The 2^{- $\Delta\Delta$ C_q} method (34) was applied to calculate the relative expression levels. The primer sequences were as follows: CAIF forward, 5'-CTTCACTCCTGCAAATGTGTT-3', reverse, 5'-TTATAG TGGGATGGGCGAGTTT-3'; miR-488-5p forward: 5'-CCC AGATAATGGCACTC-3', reverse, 5'-GAACATGTCTGC GTATCTC-3'; AVEN forward: 5'-GCGCCGGTTGAAGAT GACA-3', reverse: 5'-TGCAGAGCTAAGGAGGACACT-3'; GAPDH forward: 5'-TCGGAGTGAACGGATTTGGC-3', reverse, 5'-TGACAAGCTTCCCGTTCTCC-3'; U6 forward, 5'-AGTAAGCCCTTGCTGTCAAGTG-3' and reverse: 5'-CCT GGGTCTGATAATGCTGGG-3'.

Western blotting. Total protein was extracted from cells with RIPA buffer (Beyotime). BCA kit was used to detect protein concentration and 12% SDS-PAGE was performed to separate proteins (40 μ g) in samples. Then, the separated proteins were transferred to PVDF membranes and blocked with 5% non-fat milk at room temperature for 2 h. The proteins on PVDF membranes were labeled with primary antibodies (AVEN, ab133285, 1:800; GAPDH, ab8245, 1:2500; both Abcam) at 4°C overnight and horseradish peroxidase-conjugated secondary goat-anti-rabbit IgG (1:1,000, cat. no. ab150077, Abcam) at room temperature for 2 h. ECL kit (Beyotime Institute of Biotechnology) was used to visualize the blots. Images were recorded with the Luminescent Image Analyzer LAS-4000 system (Fujifilm) and quantified by the Gel-Pro Analyzer 4.0 software (Media Cybernetics, Inc.).

Flow cytometry. A total of ~1x10⁶ cardiomyocytes/ml were collected and centrifuged at 4°C and 710.4 g for 5 min and the culture medium was discarded. The cells were washed with 3 ml PBS and centrifuged at 4°C and 710.4 g for

5 min, cells were fixed with precooled 70% ethanol at 4°C for 2 h. Then, cells were incubated with FITC-Annexin V (300 ng/ml; 4°C) for 10 min to label apoptotic cells. The samples were further incubated with PI (Procell Life Science & Technology Co., Ltd.) at 4°C for 5 min. The apoptotic cells were detected using a Fortessa flow cytometer (BD Biosciences). FlowJo10 (BD Biosciences) was used to analyze the flow cytometry data.

Dual luciferase reporter assay. Bioinformatics analysis using mirDB (mirdb.org/) and TargetScan 7.1 (targetscan.org/vert_71/) was used to predict binding sites. The predicted binding sites of miR-488-5p on CAIF and AVEN mRNA were cloned into pGL3 luciferase reporter vector (Promega Corporation) and named CAIF-wild-type (WT) and AVEN-WT, respectively. Vectors with mutated sequences at the predicted binding sites were also synthesized and named CAIF-mutant (MUT) and AVEN-MUT, respectively. The cells were co-transfected with miR-488-5p mimics or miR-control and MUT or WT vectors using a Lipofectamine® 3000 kit (Invitrogen; Thermo Fisher Scientific, Inc.) according to the manufacturer's instructions at room temperature. TRL-SV40 vector served as an internal reference. At 48 h post-transfection, the luciferase activity was detected using a dual-luciferase assay kit and normalized to *Renilla* luciferase activity (Promega Corporation). The sequences were as follows: miR-488-5p sequences: mimic, CCCAGATAATGG CACTCTCAA; inhibitor: TTGAGAGTGCCATTATCTGGG.

2,3,5-Triphenyltetrazolium chloride (TTC) staining and evaluation of infarcted and viable myocardium. Hearts were harvested following reperfusion treatment. Perpendicular to the long axis of the heart, the heart was cut into short-axis slices (4 mm) from the apex to the bottom of the heart, then the slices were placed in a 37°C water bath within a mass fraction of 1% TTC phosphate buffer for 20 min and fixed in a volume fraction of 10% formaldehyde at room temperature for 6 h. The fixed sections were removed, dried and photographed (Canon EOS 800D).

TUNEL staining. To detect apoptotic cells in cultured myocardial cells and tissue, TUNEL staining was performed. The cells and tissue slices were fixed with paraformaldehyde (4%) at room temperature for 1 h. TUNEL kit (Sigma-Aldrich; Merck KGaA) was applied to label apoptotic cells according to the manufacturer's instruction. TUNEL staining was performed at 37°C for 2 h. PBS was used for rinsing. Then, 200 ml DAPI (1 µg/ml, Sigma-Aldrich; Merck KGaA) was applied to label nuclei at room temperature for 20 min. Neutral gum was used to mounting. Images were captured in six fields of view/sample using an inverted fluorescence microscope (Nikon Corporation; scale bar, 100 µm). The apoptotic cells were counted manually.

Reactive oxygen species (ROS) detection. 2',7'-dichlorofluorescein diacetate (DCFH) (Sigma-Aldrich; Merck KGaA) was used to detect the levels of ROS. Briefly, at the indicated time points, cardiomyocytes were rinsed with PBS (4°C). Then, the cells (3×10^4) were incubated with DCFH (10 µM) at 37°C for 30 min in the dark. The fluorescence intensity of harvested cells was detected via flow cytometry. The cells

were stimulated with 488 nm excitation light by flow cytometry. The cells were fully washed with fresh culture medium without serum three times to fully remove DCFH that did not enter the cells. The fluorescence intensity was detected on the flow cytometer within 1 h. The acquired data were analyzed with FlowJo_V10 (35).

MDA and LDH levels determination. The MDA and LDH levels of the cells were determined using Malondialdehyde (MDA) assay kit (cat. A003-1-2; Jiancheng) and Lactate dehydrogenase assay kit (cat. A020-1-2; Jiancheng) according to the instructions.

RNA pull-down assay. AmpliScribe™ T7-Flash™ Biotin-RNA Transcription kit (cat. no. ASB71110; Epicentre; Illumina, Inc.) was used to transcribe and purify biotin-labeled RNA probe *in vitro* according to manufacturer's protocol. 1×10^7 cardiomyocytes was subjected to RNA extraction using RNA extraction kit (Beyotime Institute of Biotechnology) at room temperature for 2 h. The biotin-labeled probe was incubated with 500 µl cell RNA. The mixture was incubated with streptavidin agarose beads (Invitrogen; Thermo Fisher Scientific, Inc.) at room temperature for 1 h. Following strict washing with detergent/combined buffer, the complex were collected and centrifuged at 4°C and 10,000 g for 15 min and the recovered samples were analyzed. The results were determined using RT-qPCR.

Statistical analysis. Data are expressed as the mean ± SD of three independent repeats. GraphPad 6.0 software (GraphPad Software, Inc.) was used for statistical analysis. Comparisons between two groups were performed by unpaired t-test. Comparisons between multiple groups were performed by one way ANOVA followed by post hoc Tukey's test. $P < 0.05$ was considered to indicate a statistically significant difference.

Results

CAIF expression is decreased in myocardium following I/R and in cardiomyocytes following H_2O_2 treatment. To detect whether CAIF serves a role in cardiac I/R injury, mouse I/R and oxidative stress models using H_2O_2 treated cardiomyocytes were established. RT-qPCR indicated that CAIF expression in cardiomyocytes significantly decreased from 1 h post- H_2O_2 treatment (Fig. 1A). CAIF levels in the myocardium of mice decreased during ischemia and reperfusion further inhibited its expression (Fig. 1B). These results indicated that CAIF was downregulated in MI.

CAIF overexpression inhibits H_2O_2 -induced oxidative stress injury in cardiomyocytes. MI is accompanied by oxidative stress and cardiomyocyte apoptosis (36). An oxidative stress injury model was established *in vitro* via H_2O_2 treatment. The efficiency of Ad overexpressing CAIF was assessed; RT-qPCR indicated that Ad-CAIF significantly promoted CAIF expression (Fig. 2A). Flow cytometry and TUNEL assay were performed to evaluate apoptosis of cardiomyocytes. CAIF significantly inhibited apoptosis of cardiomyocytes compared with the negative control group (Fig. 2B-D). Furthermore, release of lactate dehydrogenase (LDH) and malonaldehyde

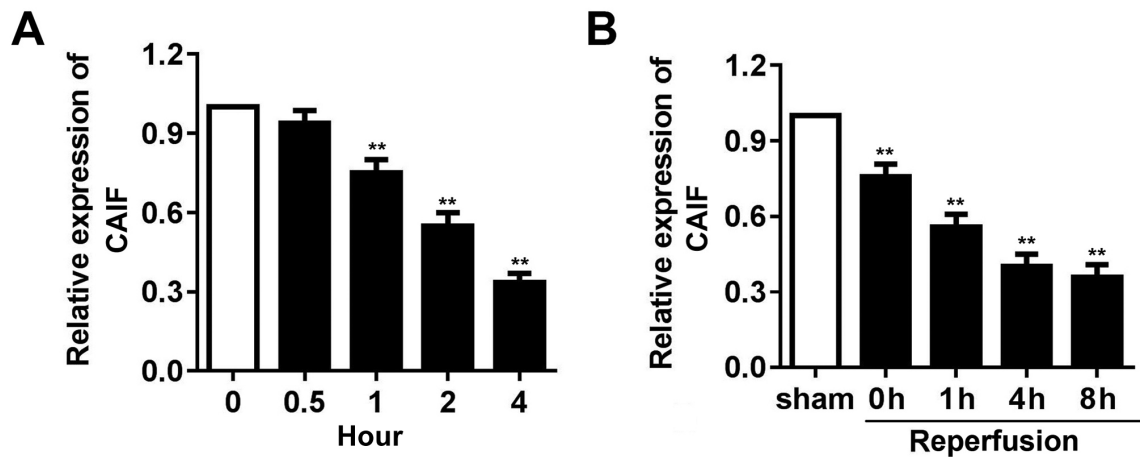


Figure 1. CAIF is downregulated in I/R injury. (A) Expression of CAIF was detected in primary mouse cardiomyocytes following H₂O₂ stimulation. **P<0.01 vs. 0 h. (B) Mice underwent I/R injury for 2 h. The expression of CAIF was detected at different time points. **P<0.01 vs. sham. CAIF, cardiac autophagy inhibitory factor; I/R, ischemia/reperfusion.

(MDA) in cell culture medium was assessed. H₂O₂ treatment significantly elevated the levels of LDH and MDA, while CAIF overexpression suppressed this (Fig. 2E and F). ROS activity was evaluated. H₂O₂ significantly promoted ROS activity of cardiomyocytes; this effect was decreased by CAIF overexpression (Fig. 2G). These results indicated that CAIF overexpression relieved the oxidative stress injury in MI.

CAIF decreases MI and apoptosis. Animals were injected with Ad-CAIF via the tail vein and I/R was performed 7 days later. RT-qPCR showed that the levels of CAIF significantly increased in the myocardium following Ad-CAIF administration (Fig. 3A). Compared with sham group, the infarct area was significantly increased in the I/R group; this effect was decreased by CAIF (Fig. 3B). TUNEL staining was used to evaluate apoptosis. CAIF significantly inhibited the I/R-induced increase in myocardium apoptosis (Fig. 3C). These results indicated that CAIF overexpression relieved MI progression *in vivo*.

CAIF sponges miR-488-5p. mirDB was used to predict the potential target genes of CAIF; the results showed that there was a complementary binding site with miR-488-5p in the sequence of CAIF (Fig. 4A). Luciferase reporter assay showed that miR-488-5p decreased the luciferase activity of cardiomyocytes transfected with reporter vector carrying CAIF-WT but not CAIF-MUT (Fig. 4B). RNA pull-down assay further demonstrated that CAIF directly bound to miR-488-5p (Fig. 4C). Expression levels of miR-488-5p were evaluated following CAIF overexpression or knockdown. The results indicated that CAIF overexpression significantly decreased miR-488-5p levels, whereas CAIF knockdown increased them (Fig. 4D). These results indicated a direct interaction between miR-488-5p and CAIF. These results indicated that miR-488-5p was negatively regulated by CAIF in MI.

miR-488-5p overexpression reverses the protective effect of CAIF. To confirm the interaction between miR-488-5p and CAIF, rescue experiments were performed. RT-qPCR indicated that miR-488-5p mimic restored expression levels

of miR-488-5p decreased by CAIF (Fig. 5A). Apoptosis assay showed that CAIF treatment decreased H₂O₂-induced cardiomyocyte apoptosis, but this effect was partially reversed by miR-488-5p overexpression (Fig. 5B-D). The levels of LDH and MDA as well as ROS activity were detected. CAIF inhibited release of LDH and MDA as well as ROS activity, while miR-488-5p partially reversed this effect (Fig. 5E-G). These results confirmed the interaction between miR-488-5p and CAIF. These results indicated that CAIF relieved the oxidative stress injury in MI via regulating miR-488-5p expression.

miR-488-5p directly targets AVEN. To elucidate the precise mechanism of CAIF and miR-488-5p in I/R injury, the downstream genes regulated by miR-488-5p were investigated. AVEN was predicted to be a potential target of miR-488-5p via Targetscan. Fig. 6A shows the binding site between miR-488-5p and CAIF. Luciferase assay showed that miR-488-5p decreased luciferase activity of cardiomyocytes transfected with reporter vector carrying AVEN-WT but not AVEN-MUT (Fig. 6B). RT-qPCR and western blotting indicated that miR-488-5p inhibited mRNA and protein expression levels of AVEN, whereas miR-488-5p promoted AVEN expression (Fig. 6C and D). RNA pull-down assay further demonstrated that AVEN can directly bound to miR-488-5p (Fig. 6E). These results indicated that miR-488-5p serves role in MI via targeting AVEN.

Discussion

MI, which is caused by blockage of coronary arteries and leads to apoptosis or necrosis of myocardial cells due to persistent ischemia and hypoxia, has one of the highest mortality rates in the world (2). Apoptosis is a process of spontaneous cell death controlled by genes (7). Following MI, myocardial cell apoptosis is an important factor leading to ventricular function weakening and myocardial remodeling (37). Therefore, inhibiting apoptosis of cardiomyocytes in the early stage of MI may effectively control its progression.

Zhuo *et al.* (38) found an association between CAIF and MI and demonstrated that lncRNAs inhibit autophagy of

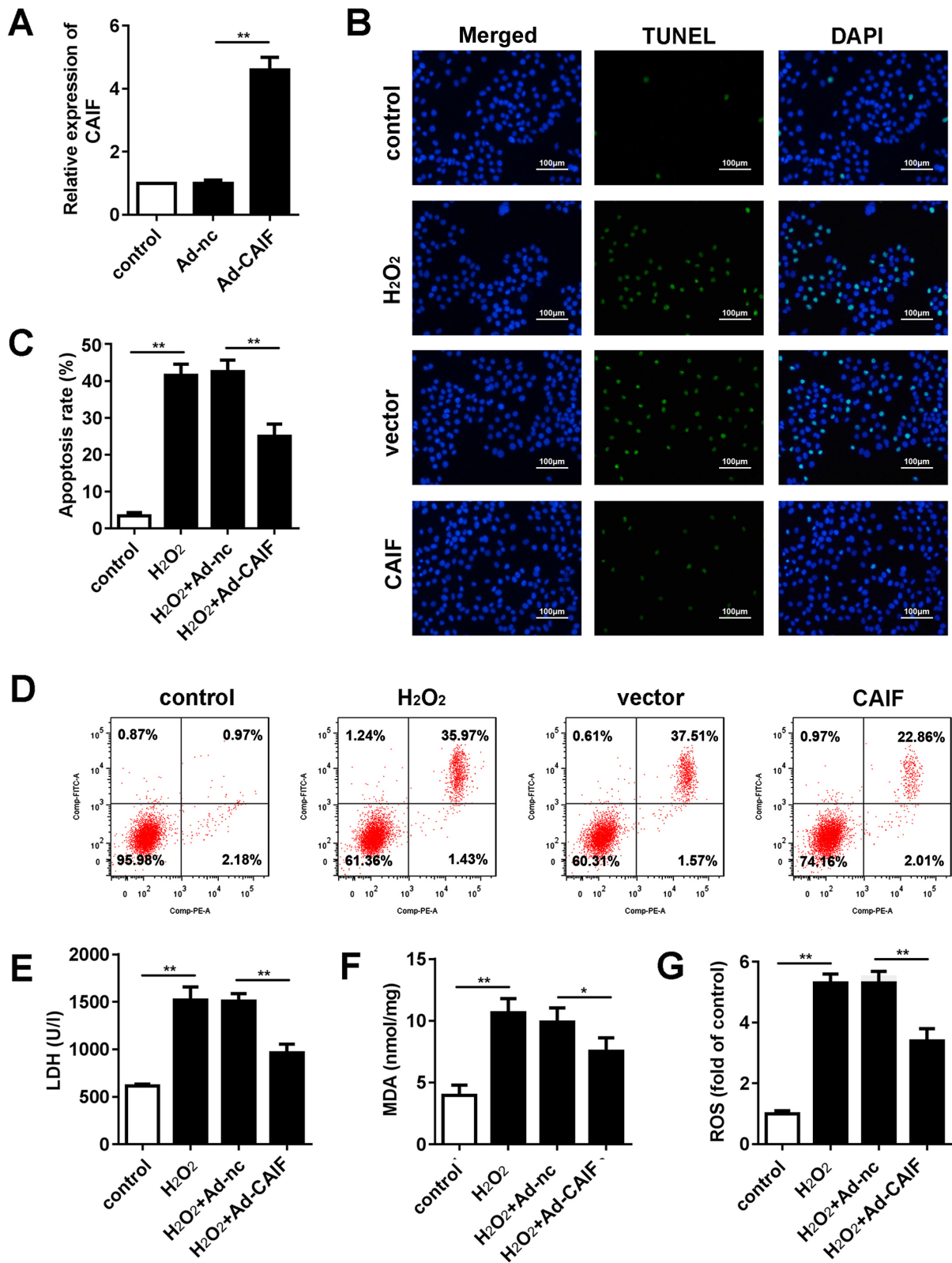


Figure 2. CAIF overexpression inhibits H₂O₂-induced apoptosis and oxidative stress of cardiomyocytes. (A) CAIF expression was detected by reverse transcription-quantitative PCR after myocardial cells were infected with Ad-CAIF. (B) Oxidative stress model was constructed using H₂O₂ treatment and apoptosis was detected by TUNEL staining. (C) Apoptosis in each group was detected by (D) flow cytometry. (E) LDH and (F) MDA content were determined by ELISA. (G) Intracellular ROS activity was determined by flow cytometry. *P<0.05 and **P<0.01. CAIF, cardiac autophagy inhibitory factor; Ad, adenovirus; LDH, lactate dehydrogenase; MDA, malonaldehyde; ROS, reactive oxygen species; nc, negative control.

myocardial cells and attenuate MI by blocking p53-mediated myocardin transcription. The expression of myocardin is upregulated by H₂O₂ and I/R and myocardin knockdown

inhibits autophagy and weakens MI. p53 regulates autophagy and myocardial I/R injury by regulating expression of myocardin (39). CAIF binds directly to p53 protein and

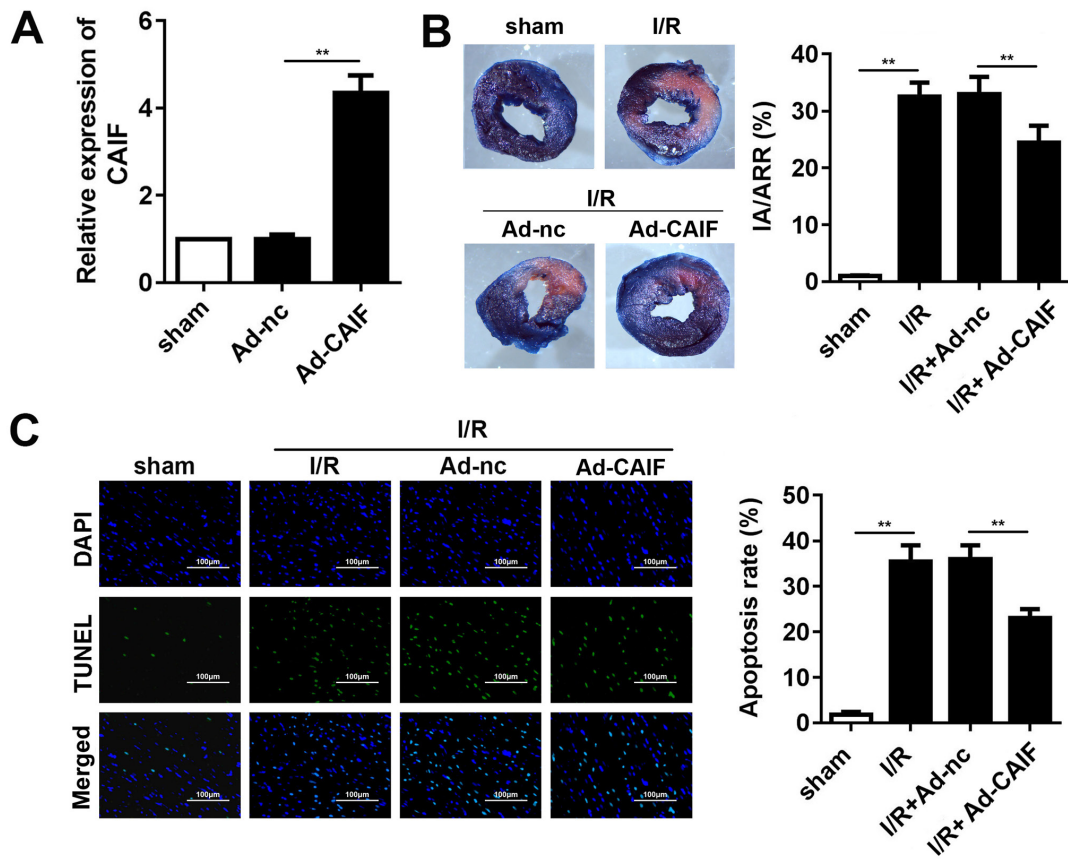


Figure 3. CAIF inhibits I/R-induced myocardium infarction and apoptosis. (A) CAIF expression was detected by reverse transcription-quantitative PCR following injection of Ad-CAIF. (B) 2,3,5-triphenyltetrazolium chloride staining was performed to detect infarct area. (C) TUNEL staining was used to detect apoptosis of cardiomyocytes. Magnification, $\times 100$. $^{**}P < 0.01$. CAIF, cardiac autophagy inhibitory factor; Ad, adenovirus; I/R, ischemia/reperfusion; nc, negative control; IA/ARR, infarct area/area at risk.

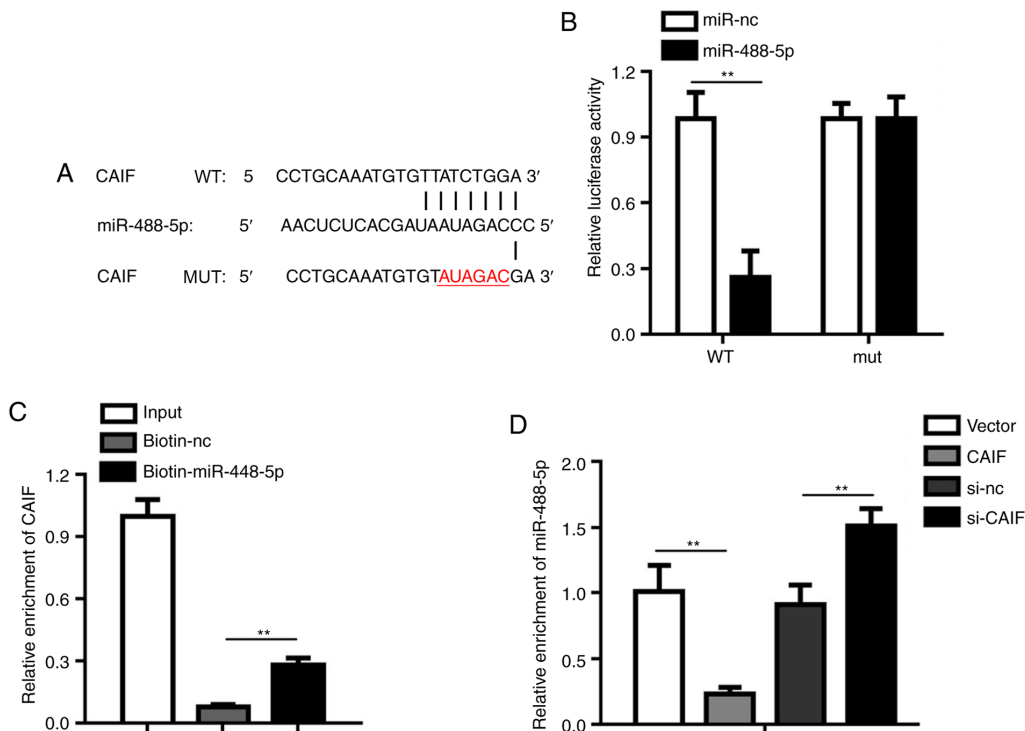


Figure 4. CAIF sponges miR-488-5p. (A) MUT Binding site (red) between CAIF and miR-488-5p. (B) Luciferase reporter experiment was performed to detect binding between CAIF and miR-488-5p. (C) RNA pull-down assay was performed to confirm the interaction between CAIF and miR-488-5p. (D) Reverse transcription-quantitative PCR was used to detect the expression of miR-488-5p. $^{**}P < 0.01$. CAIF, cardiac autophagy inhibitory factor; miR, microRNA; WT, wild-type; MUT, mutant; nc, negative control; si, small interfering.

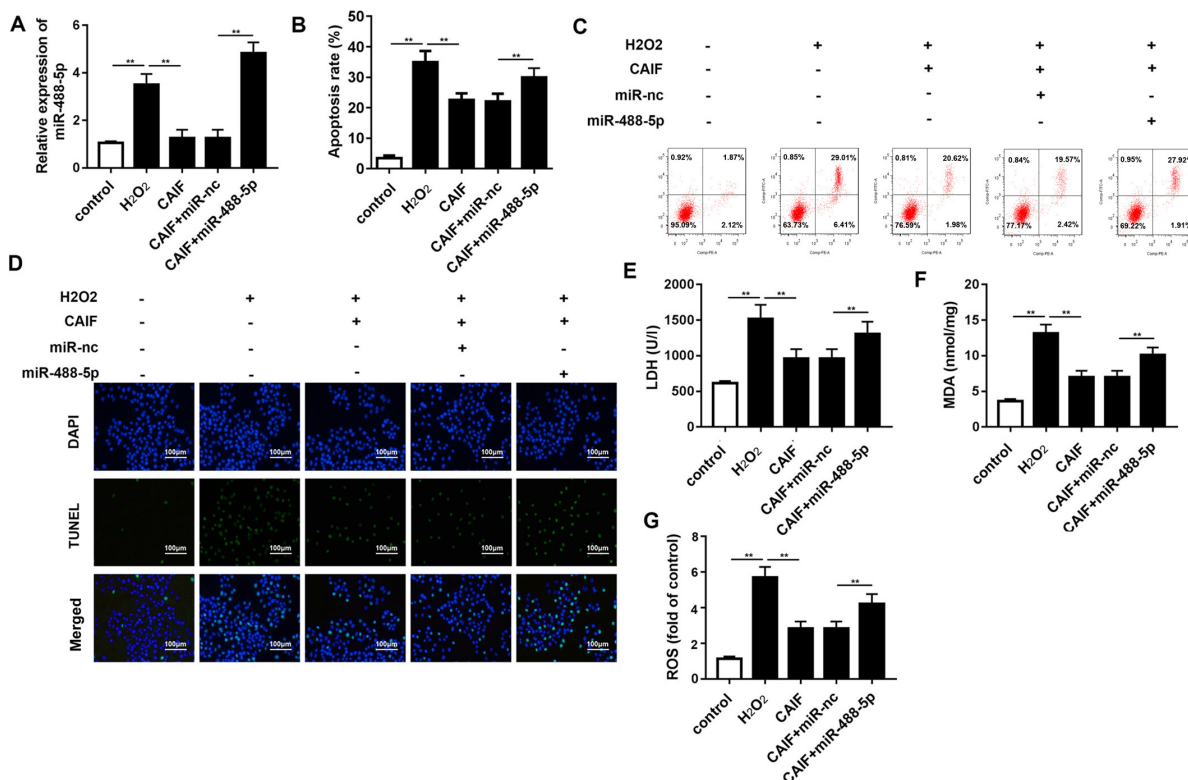


Figure 5. miR-488-5p reverses the effect of CAIF on cardiac ischemia/reperfusion injury. (A) Detection of miR-488-5p expression via reverse transcription-quantitative PCR. (B) Apoptosis of cardiomyocytes was detected by (C) flow cytometry. (D) TUNEL staining of the cardiomyocytes. (E) LDH and (F) MDA content were determined by ELISA. (G) ROS activity was assessed by flow cytometry. **P<0.01. CAIF, cardiac autophagy inhibitory factor; miR, microRNA; LDH, lactate dehydrogenase; MDA, malonaldehyde; ROS, reactive oxygen species; nc, negative control.

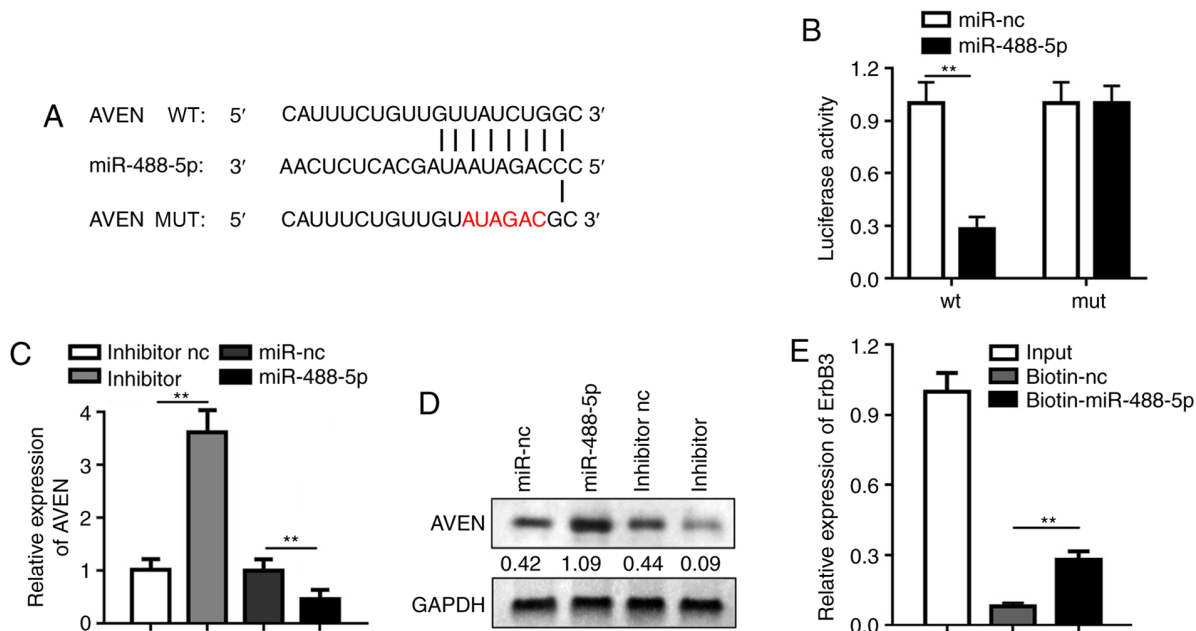


Figure 6. miR-488-5p targets AVEN directly. (A) Binding site (red) between miR-488-5p and AVEN. (B) Luciferase reporter experiment was performed to detect binding between AVEN and miR-488-5p. (C) Reverse transcription-quantitative PCR and (D) western blotting were used to detect mRNA and protein expression levels of miR-488-5p, respectively. (E) RNA pull-down assay was performed to confirm the interaction between AVEN and miR-488-5p. **P<0.01. miR, microRNA; AVEN, apoptosis and caspase activation inhibitor; WT, wild-type; MUT, mutant; nc, negative control.

blocks p53-mediated myocardin transcription, which leads to decreased myocardin expression (40,41). Myocardial cell apoptosis and oxidative stress are involved in a series of

pathological changes, including ventricular remodeling and heart failure, following MI (42-44). Among these, myocardial cell apoptosis is an important factor in MI, which leads to

the infarction but also promotes myocardial remodeling (45). In the present study, CAIF inhibited the infarct area and apoptosis of cardiomyocytes *in vivo*, and protected cultured cardiomyocytes from H₂O₂-induced apoptosis.

lncRNAs serve as sponges of miRNA molecules, binding with miRNA via endogenous competition to inhibit degradation of mRNA (46,47). Abnormally expressed miRNAs are widely used in clinical diagnosis and treatment of tumors. miRNAs affect cardiovascular development, diseases and other pathophysiological processes (48,49) by regulating cell differentiation, migration and proliferation. In the present study, miR-488-5p was sponged by CAIF in MI, indicating that miRNAs serve an important role in MI and may be a promising research direction. To the best of our knowledge, the number of studies of miR-488-5p is low. miR-488-5p is expressed at low levels and sponged by small nucleolar host gene 1 in acute myeloid leukemia (50). In addition, miR-488-5p acts as a tumor suppressor and is lost during melanoma development (51).

miRNAs target downstream mRNAs to inhibit their expression, thus participating in the regulation of cell processes. For example, downregulated miR-26a-5p induced the apoptosis of endothelial cells in coronary heart disease via targeting PTEN (52). MiR-103b promoted apoptosis in stored platelets via targeting ITGB3 (53). Here, bioinformatics analysis predicted AVEN as a potential target of miR-488-5p. AVEN binds with the apoptosis regulator Bcl-xL and Apaf-1 (29). AVEN impairs Apaf-1-mediated activation of caspases, thus inhibiting proteolytic activation of caspases and suppressing apoptosis. Moreover, a previous study indicated that AVEN is involved in hypoxia-induced cardiomyocyte injury as a target gene of miR-30b-5p (54). However, the present study did not perform rescue experiments to confirm the interaction between AVEN and miR-488-5p and CAIF; this should be assessed in future.

In conclusion, the present study observed downregulated CAIF in the myocardium and cardiomyocytes following I/R and H₂O₂ treatment, respectively. CAIF inhibited I/R injury via the miR-488-5p/AVEN signaling axis. It remains to be verified whether the diagnostic and therapeutic potential of CAIF can be applied to clinical treatment.

Acknowledgements

Not applicable.

Funding

No funding was received.

Availability of data and materials

The datasets used and/or analyzed during the current study are available from the corresponding author on reasonable request.

Authors' contributions

XL and RC performed *in vitro* experiments. XL and LW performed *in vivo* experiments. ZL performed bioinformatics analysis. YL performed statistical analysis. DT designed the study and wrote the manuscript. XL and DT confirm the

authenticity of all the raw data. All authors have read and approved the final manuscript.

Ethics approval and consent to participate

The study was approved by the Ethics Committee of Guilin People's Hospital.

Patient consent for publication

Not applicable.

Competing interests

The authors declare that they have no competing interests.

References

- Barnett R: Acute myocardial infarction. *Lancet* 393: 2580, 2019.
- Ketchum ES, Dickstein K, Kjekshus J, Pitt B, Wong MF, Linker DT and Levy WC: The seattle post myocardial infarction model (SPIM): Prediction of mortality after acute myocardial infarction with left ventricular dysfunction. *Eur Heart J Acute Cardiovasc Care* 3: 46-55, 2014.
- De Villiers C and Riley PR: Mouse models of myocardial infarction: Comparing permanent ligation and ischaemia-reperfusion. *Dis Model Mech* 13: dmm046565, 2020.
- Blankenberg S, Neumann JT and Westermann D: Diagnosing myocardial infarction: A highly sensitive issue. *Lancet* 392: 893-894, 2018.
- Isaaz K and Gerbay A: Deferred stenting in acute ST elevation myocardial infarction. *Lancet* 388: 1371, 2016.
- Hombach S and Kretz M: Non-coding RNAs: Classification, biology and functioning. *Adv Exp Med Biol* 937: 3-17, 2016.
- Yu BY and Dong B: lncRNA H19 regulates cardiomyocyte apoptosis and acute myocardial infarction by targeting miR-29b. *Int J Cardiol* 271: 25, 2018.
- Yin Y, Lv L and Wang W: Expression of miRNA-214 in the sera of elderly patients with acute myocardial infarction and its effect on cardiomyocyte apoptosis. *Exp Ther Med* 17: 4657-4662, 2019.
- Xin B, Liu Y, Li G, Xu Y and Cui W: The role of lncRNA SNHG16 in myocardial cell injury induced by acute myocardial infarction and the underlying functional regulation mechanism. *Panminerva Med* 63: 388-389, 2019.
- Zhang Y, Jiao L, Sun L, Li Y, Gao Y, Xu C, Shao Y, Li M, Li C, Lu Y, *et al*: lncRNA ZFAS1 as a SERCA2a inhibitor to cause intracellular Ca(2+) overload and contractile dysfunction in a mouse model of myocardial infarction. *Circ Res* 122: 1354-1368, 2018.
- Liao J, He Q, Li M, Chen Y, Liu Y and Wang J: lncRNA MIAT: Myocardial infarction associated and more. *Gene* 578: 158-161, 2016.
- Hao K, Lei W, Wu H, Wu J, Yang Z, Yan S, Lu XA, Li J, Xia X, Han X, *et al*: lncRNA-Safe contributes to cardiac fibrosis through Safe-Sfrp2-HuR complex in mouse myocardial infarction. *Theranostics* 9: 7282-7297, 2019.
- Viereck J, Bührke A, Foinquinos A, Chatterjee S, Kleeberger JA, Xiao K, Janssen-Peters H, Batkai S, Ramanujam D, Kraft T, *et al*: Targeting muscle-enriched long non-coding RNA H19 reverses pathological cardiac hypertrophy. *Eur Heart J* 41: 3462-3474, 2020.
- Yang J, Huang X, Hu F, Fu X, Jiang Z and Chen K: lncRNA ANRIL knockdown relieves myocardial cell apoptosis in acute myocardial infarction by regulating IL-33/ST2. *Cell Cycle* 18: 3393-3403, 2019.
- Yu SY, Dong B, Fang ZF, Hu XQ, Tang L and Zhou SH: Knockdown of lncRNA AK139328 alleviates myocardial ischaemia/reperfusion injury in diabetic mice via modulating miR-204-3p and inhibiting autophagy. *J Cell Mol Med* 22: 4886-4898, 2018.
- Wang SM, Liu GQ, Xian HB, Si JL, Qi SX and Yu YP: lncRNA NEAT1 alleviates sepsis-induced myocardial injury by regulating the TLR2/NF-κB signaling pathway. *Eur Rev Med Pharmacol Sci* 23: 4898-4907, 2019.

17. Wang Y and Zhang Y: LncRNA CAIF suppresses LPS-induced inflammation and apoptosis of cardiomyocytes through regulating miR-16 demethylation. *Immun Inflamm Dis* 9: 1468-1478, 2021.
18. Liu CY, Zhang YH, Li RB, Zhou LY, An T, Zhang RC, Zhai M, Huang Y, Yan KW, Dong YH, *et al*: LncRNA CAIF inhibits autophagy and attenuates myocardial infarction by blocking p53-mediated myocardial transcription. *Nat Commun* 9: 29, 2018.
19. Leads from the MMWR. Recommendations for protection against viral hepatitis. *JAMA* 254: 197-198, 1985.
20. Cramer DW and Elias KM: A prognostically relevant miRNA signature for epithelial ovarian cancer. *Lancet Oncol* 17: 1032-1033, 2016.
21. Krell J, Stebbing J, Frampton AE, Carissimi C, Harding V, De Giorgio A, Fulci V, Macino G, Colombo T and Castellano L: The role of TP53 in miRNA loading onto AGO2 and in remodelling the miRNA-mRNA interaction network. *Lancet* 385 (Suppl 1): S15, 2015.
22. Feng R, Sang Q, Zhu Y, Fu W, Liu M, Xu Y, Shi H, Xu Y, Qu R, Chai R, *et al*: MiRNA-320 in the human follicular fluid is associated with embryo quality in vivo and affects mouse embryonic development in vitro. *Sci Rep* 5: 8689, 2015.
23. Collignon J: miRNA in embryonic development: The taming of Nodal signaling. *Dev Cell* 13: 458-460, 2007.
24. Zhong YX, Li WS, Liao LS and Liang L: LncRNA CCAT1 promotes cell proliferation and differentiation via negative modulation of miRNA-218 in human DPSCs. *Eur Rev Med Pharmacol Sci* 23: 3575-3583, 2019.
25. Hara ES, Ono M, Eguchi T, Kubota S, Pham HT, Sonoyama W, Tajima S, Takigawa M, Calderwood SK and Kuboki T: miRNA-720 controls stem cell phenotype, proliferation and differentiation of human dental pulp cells. *PLoS One* 8: e83545, 2013.
26. Shen N, Liu S, Cui J, Li Q, You Y, Zhong Z, Cheng F, Guo AY, Zou P, Yuan G and Zhu X: Tumor necrosis factor α knockout impaired tumorigenesis in chronic myeloid leukemia cells partly by metabolism modification and miRNA regulation. *Oncotargets Ther* 12: 2355-2364, 2019.
27. Wu A, Lou L, Zhai J, Zhang D, Chai L, Nie B, Zhu H, Gao Y, Shang H and Zhao M: miRNA expression profile and effect of Wenxin granule in rats with ligation-induced myocardial infarction. *Int J Genomics* 2017: 2175871, 2017.
28. Wang ZH, Sun XY, Li CL, Sun YM, Li J, Wang LF and Li ZQ: miRNA-21 expression in the serum of elderly patients with acute myocardial infarction. *Med Sci Monit* 23: 5728-5734, 2017.
29. Zhang L and Jia X: Down-regulation of miR-30b-5p protects cardiomyocytes against hypoxia-induced injury by targeting Aven. *Cell Mol Biol Lett* 24: 61, 2019.
30. American Veterinary Medical Association: AVMA guidelines for complementary and alternative veterinary medicine. *J Am Vet Med Assoc* 218: 1731, 2001.
31. Zeng J, Zhu L, Liu J, Zhu T, Xie Z, Sun X and Zhang H: Metformin protects against oxidative stress injury induced by ischemia/reperfusion via regulation of the lncRNA-H19/miR-148a-3p/Rock2 axis. *Oxid Med Cell Longev* 2019: 8768327, 2019.
32. Dhalla NS, Elmoselhi AB, Hata T and Makino N: Status of myocardial antioxidants in ischemia-reperfusion injury. *Cardiovasc Res* 47: 446-456, 2000.
33. Yang D, Yu J, Liu HB, Yan XQ, Hu J, Yu Y, Guo J, Yuan Y and Du ZM: The long non-coding RNA TUG1-miR-9a-5p axis contributes to ischemic injuries by promoting cardiomyocyte apoptosis via targeting KLF5. *Cell Death Dis* 10: 908, 2019.
34. Livak KJ and Schmittgen TD: Analysis of relative gene expression data using real-time quantitative PCR and the 2(-Delta Delta C(T)) method. *Methods* 25: 402-408, 2001.
35. Kroeze A, van Hoven V, Verheij MW, Turksma AW, Weterings N, van Gassen S, Zeerleder SS, Blom B, Voermans C and Hazenberg MD: Presence of innate lymphoid cells in allogeneic hematopoietic grafts correlates with reduced graft-versus-host disease. *Cytotherapy* 24: 302-310, 2022.
36. Yoshimura C, Nagasaka A, Kurose H and Nakaya M: Efferocytosis during myocardial infarction. *J Biochem* 168: 1-6, 2020.
37. González A, Fortuño MA, Querejeta R, Ravassa S, López B, López N and Díez J: Cardiomyocyte apoptosis in hypertensive cardiomyopathy. *Cardiovasc Res* 59: 549-562, 2003.
38. Zhuo LA, Wen YT, Wang Y, Liang ZF, Wu G, Nong MD and Miao L: LncRNA SNHG8 is identified as a key regulator of acute myocardial infarction by RNA-seq analysis. *Lipids Health Dis* 18: 201, 2019.
39. Su Q, Lv XW, Xu YL, Cai RP, Dai RX, Yang XH, Zhao WK and Kong BH: Exosomal LINC00174 derived from vascular endothelial cells attenuates myocardial I/R injury via p53-mediated autophagy and apoptosis. *Mol Ther Nucleic Acids* 23: 1304-1322, 2021.
40. Zhou T, Qin G, Yang L, Xiang D and Li S: LncRNA XIST regulates myocardial infarction by targeting miR-130a-3p. *J Cell Physiol* 234: 8659-8667, 2019.
41. Zhang G, Sun H, Zhang Y, Zhao H, Fan W, Li J, Lv Y, Song Q, Li J, Zhang M and Shi H: Characterization of dysregulated lncRNA-mRNA network based on ceRNA hypothesis to reveal the occurrence and recurrence of myocardial infarction. *Cell Death Discov* 4: 35, 2018.
42. Sun F, Zhuang Y, Zhu H, Wu H, Li D, Zhan L, Yang W, Yuan Y, Xie Y, Yang S, *et al*: LncRNA PCFL promotes cardiac fibrosis via miR-378/GRB2 pathway following myocardial infarction. *J Mol Cell Cardiol* 133: 188-198, 2019.
43. Zhang Y, Hou YM, Gao F, Xiao JW, Li CC and Tang Y: lncRNA GAS5 regulates myocardial infarction by targeting the miR-525-5p/CALM2 axis. *J Cell Biochem* 120: 18678-186788, 2019.
44. Su T, Shao X, Zhang X, Yang C and Shao X: Value of circulating miRNA-1 detected within 3 h after the onset of acute chest pain in the diagnosis and prognosis of acute myocardial infarction. *Int J Cardiol* 307: 146-151, 2020.
45. Yaoita H, Ogawa K, Maehara K and Maruyama Y: Apoptosis in relevant clinical situations: Contribution of apoptosis in myocardial infarction. *Cardiovasc Res* 45: 630-641, 2000.
46. Song Y, Zhang C, Zhang J, Jiao Z, Dong N, Wang G, Wang Z and Wang L: Localized injection of miRNA-21-enriched extracellular vesicles effectively restores cardiac function after myocardial infarction. *Theranostics* 9: 2346-2360, 2019.
47. Fan PC, Chen CC, Peng CC, Chang CH, Yang CH, Yang C, Chu LJ, Chen YC, Yang CW, Chang YS and Chu PH: A circulating miRNA signature for early diagnosis of acute kidney injury following acute myocardial infarction. *J Transl Med* 17: 139, 2019.
48. Bejerano T, Etzion S, Elyagon S, Etzion Y and Cohen S: Nanoparticle delivery of miRNA-21 mimic to cardiac macrophages improves myocardial remodeling after myocardial infarction. *Nano Lett* 18: 5885-5891, 2018.
49. Gidlöf O, van der Brug M, Ohman J, Gilje P, Olde B, Wahlestedt C and Erlinge D: Platelets activated during myocardial infarction release functional miRNA, which can be taken up by endothelial cells and regulate ICAM1 expression. *Blood* 121: 3908-3917, S1-S26, 2013.
50. Bao XL, Zhang L and Song WP: LncRNA SNHG1 overexpression regulates the proliferation of acute myeloid leukemia cells through miR-488-5p/NUP205 axis. *Eur Rev Med Pharmacol Sci* 23: 5896-5903, 2019.
51. Arnold J, Engelmann JC, Schneider N, Bossert AK and Kuphal S: miR-488-5p and its role in melanoma. *Exp Mol Pathol* 112: 104348, 2020.
52. Jing R, Zhong QQ, Long TY, Pan W and Qian ZX: Downregulated miRNA-26a-5p induces the apoptosis of endothelial cells in coronary heart disease by inhibiting PI3K/AKT pathway. *Eur Rev Med Pharmacol Sci* 23: 4940-4947, 2019.
53. Dahiya N and Atreya C: MiRNA-103b downregulates ITGB3 and mediates apoptosis in ex vivo stored human platelets. *Microna* 10: 123-129, 2021.
54. Melzer IM, Fernández SB, Bösser S, Lohrig K, Lewandrowski U, Wolters D, Kehrlöesser S, Brezniceanu ML, Theos AC, Irusta PM, *et al*: The Apaf-1-binding protein aven is cleaved by cathepsin D to unleash its anti-apoptotic potential. *Cell Death Differ* 19: 1435-1445, 2012.



This work is licensed under a Creative Commons Attribution 4.0 International (CC BY-NC 4.0) License